

# Efficient dynamic nuclear polarization of phosphorus in silicon in strong magnetic fields and at low temperatures

J. Järvinen,<sup>1,\*</sup> J. Ahokas,<sup>1</sup> S. Sheludiyakov,<sup>1</sup> O. Vainio,<sup>1</sup> L. Lehtonen,<sup>1</sup> S. Vasiliev,<sup>1</sup> D. Zvezdov,<sup>1,2</sup> Y. Fujii,<sup>3</sup> S. Mitsudo,<sup>3</sup> T. Mizusaki,<sup>3</sup> M. Gwak,<sup>4</sup> SangGap Lee,<sup>4</sup> Soonchil Lee,<sup>5</sup> and L. Vlasenko<sup>6</sup>

<sup>1</sup>*Wihuri Physical Laboratory, Department of Physics and Astronomy, University of Turku, 20014 Turku, Finland*

<sup>2</sup>*Institute of Physics, Kazan Federal University, Russia*

<sup>3</sup>*Research Center for Development of Far-Infrared Region, University of Fukui, 3-9-1 Bunkyo, Fukui 910-8507, Japan*

<sup>4</sup>*Division of Materials Science, Korea Basic Science Institute, 169-148 Gwahak-ro, Yuseong-gu, Daejeon 305-806, Korea*

<sup>5</sup>*Department of Physics, Korea Advanced Institute of Science and Technology, 291 Daehak-ro, Yuseong-gu, Daejeon 305-701, Korea*

<sup>6</sup>*A. F. Ioffe Physico-Technical Institute, Russian Academy of Sciences, 194021 St. Petersburg, Russia*

(Received 12 March 2014; revised manuscript received 3 September 2014; published 1 December 2014)

Efficient manipulation of nuclear spins is important for utilizing them as qubits for quantum computing. In this work we report record high polarizations of <sup>31</sup>P and <sup>29</sup>Si nuclear spins in P-doped silicon in a strong magnetic field (4.6 T) and at temperatures below 1 K. We reached <sup>31</sup>P nuclear polarization values exceeding 98% after 20 min of pumping the high-field electron spin resonance (ESR) line with a very small microwave power of 0.4  $\mu$ W. We evaluate that the ratio of the hyperfine-state populations increases by three orders of magnitude after 2 hours of pumping, and an extremely pure nuclear spin state can be created, with less than 0.01 ppb impurities. A negative dynamic nuclear polarization has been observed by pumping the low-field ESR line of <sup>31</sup>P followed by the flip-flip cross relaxation, the transition which is fully forbidden for isolated donors. We estimate that while pumping the ESR transitions of <sup>31</sup>P also the nuclei of <sup>29</sup>Si get polarized, and polarization exceeding 60% has been obtained. We performed measurements of relaxation rates of flip-flop and flip-flip transitions which turned out to be nearly temperature independent. Temperature dependence of the <sup>31</sup>P nuclear relaxation was studied down to 0.75 K, below which the relaxation time became too long to be measured. We found that the polarization evolution under pumping and during relaxation deviates substantially from a simple exponential function of time. We suggest that the nonexponential polarization dynamics of <sup>31</sup>P donors is mediated by the orientation of <sup>29</sup>Si nuclei, which affect the transition probabilities of the forbidden cross-relaxation processes.

DOI: [10.1103/PhysRevB.90.214401](https://doi.org/10.1103/PhysRevB.90.214401)

PACS number(s): 76.70.-r, 71.55.Cn, 76.30.-v, 76.60.Es

## I. INTRODUCTION

Shallow donors P, As, and Bi in silicon have been studied extensively since the pioneering experiments of Feher [1]. A revived interest in these systems has been raised by a recent proposal of using donor spins as qubits for quantum computing [2]. A long coherence time and ease of qubit initialization by external microwave fields are necessary conditions for building a quantum computer. These properties, also known as long transversal relaxation time and fast dynamic nuclear polarization, are inherent features of P impurities in Si (Si:P) at cryogenic temperatures. This work is concerned with the dynamic nuclear polarization and relaxation of P donors in silicon at low temperatures and high magnetic fields, when their electron spins are polarized to a very high degree, while the nuclear spins are not yet polarized.

The Overhauser effect (OE) is one of the well-known and effective ways of dynamic nuclear polarization (DNP). In the OE the allowed electron spin resonance transitions are saturated, and the subsequent cross relaxation with the simultaneous spin flips of electron and nucleus leads to the population transfer from one nuclear state to another. Efficiency of the OE DNP depends on the possibility of saturating the allowed transitions and on the subsequent cross-relaxation rate via so-called forbidden transitions. While the thermal equilibrium polarization increases exponentially

with increasing magnetic field and decreasing temperature due to the Boltzmann factor, magnetic field dependence of OE DNP involves several complicated factors and it is not obvious whether its efficiency will improve in strong magnetic fields [3].

There are two possible types of cross relaxation via the flip-flop and flip-flip transitions, in which the electron and nuclear spins flip in opposite or the same directions, respectively. Both transition probabilities strongly depend on the anisotropy of the interaction between electron and nucleus. Dipole-dipole interaction between the host lattice nuclei and donor electron has large anisotropy which ensures fast relaxation rate. Due to this reason the OE DNP has been successfully utilized for polarizing nuclei in solids and liquids via embedded paramagnetic ions (see [3,4] for recent reviews). The situation is different for the own (core) nuclei of the donors. Although hyperfine interaction is much stronger in this case, it is of isotropic Fermi type unless the electron cloud is strongly distorted by the crystalline field. The thermal relaxation via the forbidden transitions may be caused by the oscillating magnetic fields resulting from the modulation of the internal dipolar or hyperfine interaction by the lattice vibrations [5,6]. In the first case the probabilities of the forbidden transitions are reduced from that of the allowed transitions by the square of the hyperfine mixing factor  $\eta^2 = (A/2\hbar\gamma_e B_0)^2$ , a very large factor in strong fields [5,6]. Here  $A$  is the hyperfine constant,  $\gamma_e$  is the electron gyromagnetic ratio, and  $B_0$  is applied static magnetic field. The flip-flip transition is fully forbidden in the case of isotropic

\*jaanja@utu.fi

hyperfine interactions. However, the second relaxation channel due to the modulation of hyperfine interaction may provide relaxation rates of forbidden transitions comparable to the allowed transitions rates [6]. This mechanism could ensure high OE DNP rate in strong magnetic fields.

A second important factor influencing the efficiency of DNP is the nuclear relaxation rate, which returns the polarization to thermal equilibrium. The main relaxation mechanism at low temperatures is the nuclear Orbach process, which also involves the flip-flop and flip-flip transitions with the rate proportional to the Boltzmann factor  $\exp(-\hbar\gamma_e B/k_B T)$  [7]. At low temperatures the nuclear relaxation rate decreases exponentially, increasing the efficiency of the OE DNP.

DNP in high fields and low temperatures has been extensively studied in the field of nuclear physics, aiming at high polarization of nuclear targets of various materials. Proton polarizations close to 100% and deuteron polarization exceeding 50% were reported [8]. P in silicon, however, has not been thoroughly investigated in strong magnetic fields and we are not aware of any works below 1 K. The highest  $^{31}\text{P}$  DNP value of  $\approx 75\%$  has been reached in 8.6 T magnetic field [9] and at temperatures of  $\approx 3$  K. The nuclear relaxation rate turned out to be fast in these conditions which, regardless of the high electron spin polarization ( $>98\%$ ), limited reaching a higher nuclear polarization. DNP via the flip-flip transition was considered to be impossible in this work.

Typically in DNP experiments relatively high values of microwave power (up to 1 W) were used for irradiating Si:P samples. The reason is the necessity of saturating the allowed transitions, which efficiency is limited by the spin-lattice relaxation of electrons. The rate of this relaxation may strongly depend on magnetic field following the  $B_0^4$  dependence [3,10].

In the present work we demonstrate that the efficiency of OE DNP is very high in strong magnetic fields and low temperatures. We cooled Si:P samples to  $\approx 0.2$  K, which led to a decrease of the  $^{31}\text{P}$  nuclear relaxation rate to immeasurably small values. The nuclear polarization  $P \geq 0.98$  was achieved after 20 minutes of excitation. We suggest that extremely pure nuclear spin states with  $1 - P < 10^{-11}$  can be produced with sub- $\mu\text{W}$  power levels. We evaluated the cross relaxation rate by measuring the rate of the OE DNP, in which the flip-flop transition is the limiting step. We present data on the measurements of nuclear relaxation of  $^{31}\text{P}$  as a function of temperature.

## II. EXPERIMENTAL DETAILS

The experimental cell (SC) with the Si:P sample was placed in the center of a superconductive magnet producing a field of 4.6 T and cooled down by a dilution refrigerator (Fig. 1). The sample of crystalline silicon with natural abundance,  $2 \times 2 \times 0.07$  mm in size and doped by  $6.5 \times 10^{16} \text{ cm}^{-3}$  of P, was placed onto the flat mirror of a Fabry-Perot resonator (FPR) having a  $Q$  of approximately 4000. The crystal's [111] axis was directed along the axis of the FPR resonator and polarizing magnetic field. Electron spin resonance (ESR) spectra from the sample were detected with a cryogenic heterodyne spectrometer [11] operating at 128 GHz. The spectrometer provides both absorption and dispersion signal components without a modulation of the magnetic field and

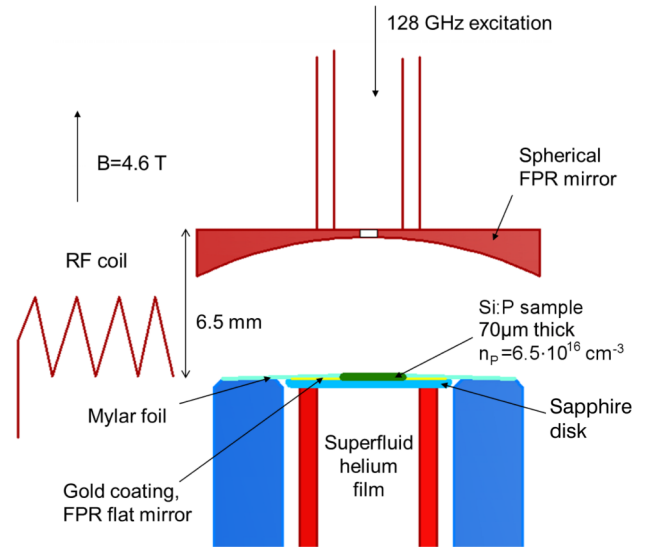


FIG. 1. (Color online) Scheme of the experimental setup with Fabry-Perot resonator.

is optimized for reaching high sensitivity at a small excitation power. This is important when studying samples with long electron spin-lattice relaxation times ( $T_{1e} \approx 0.2$  s in our case). To avoid the saturation of Si:P ESR lines below 1 K we had to use a very low microwave power for *detection*, typically below 1  $\mu\text{W}$ . For pumping the ESR lines in the DNP experiments we used the maximum available microwave power of 0.4  $\mu\text{W}$ , which will be further referred to as *pumping* power. An additional low-frequency RF coil has been fixed at the side of the FPR. The RF field of the coil is weakly coupled to the silicon sample, but due to slow nuclear relaxation can be effectively used for saturation of the nuclear transitions. In this work we used the coil for saturation of  $^{29}\text{Si}$  nuclear transitions at 38.9 MHz.

Cooling of the sample to 100 mK could be problematic because of the very large Kapitza resistance between the sample and the metal surface. Thermal contact of the sample was improved with a superfluid helium. The flat mirror with the sample was isolated from the main vacuum by a Mylar foil to a separate chamber, which could be filled with liquid helium (Fig. 1). However, in this work, we did not observe any significant difference in the thermalization of Si:P samples with or without helium film at temperatures above 500 mK.

## III. RESULTS

### A. Dynamic nuclear polarization of $^{31}\text{P}$

The CW ESR absorption spectrum of a Si:P sample recorded just after cooling down to a low temperature is shown in the upper trace of Fig. 2. The spectrum consists of two lines corresponding to the allowed  $a$ - $d$  (low field) and  $b$ - $c$  (high field) transitions, separated by  $\approx 42$  G due to the hyperfine interaction of the  $^{31}\text{P}$  electron with its own nucleus. The lines are inhomogeneously broadened by the spin-1/2  $^{29}\text{Si}$  nuclei of the host lattice which reside inside the relatively disperse electron cloud of the  $^{31}\text{P}$  electron [1].

First, we performed a DNP experiment by saturating the allowed  $b$ - $c$  transition. The magnetic field was set to

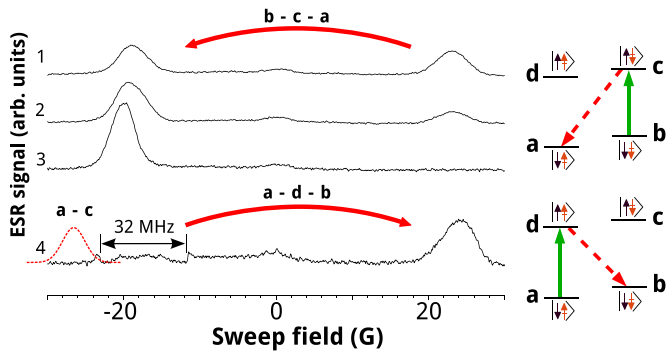


FIG. 2. (Color online) The ESR absorption spectra demonstrating DNP of P in silicon. Traces 1, 2, and 3 demonstrate the Overhauser effect: pumping the  $b$ - $c$  transition, followed by the forbidden  $c$ - $a$  relaxation. Trace 1, before pumping; trace 2, after 100 s pumping; trace 3, after 20 min pumping. Trace 4 demonstrates the result of pumping  $a$ - $d$  transition with the relaxation via the  $d$ - $b$  transition. Position of the forbidden  $a$ - $c$  transition is marked with the dashed line. The transfer of hyperfine level populations is shown in the level diagram on the right. Solid arrows denote the allowed ESR transitions and dashed traces relaxations via the forbidden flip-flop (upper diagram) and flip-flip (lower diagram) transitions.

the center of the  $b$ - $c$  line and the excitation power was increased to the pumping value, aiming at full saturation of the ESR transition. For increasing the efficiency of the DNP the ESR excitation frequency was modulated with the frequency deviation corresponding to 3–4 linewidths and with the modulation rate of 10–20 Hz. Since the electron spin-lattice relaxation time  $\approx 0.2$  s is substantially longer than the modulation period, all the spin packets in the ESR line are simultaneously saturated. After pumping the  $b$ - $c$  transition for a time  $t_p$ , the spectrometer was switched to detection power, and undistorted spectra with both ESR lines were recorded. Then, the nuclear polarization  $P(t) = (n_a - n_b)/(n_a + n_b)$  was calculated from the ESR absorption line areas, which are proportional to the populations  $n_a$  and  $n_b$  of the  $a$  and  $b$  states. The polarization measurement was performed shortly ( $< 50$  s) after the pumping, so that the nuclear-state populations were not influenced by the nuclear relaxation, which turned out to be very slow below 1 K.

The spectra after  $t_p = 30$  s and  $t_p = 20$  min are shown in the second and third traces of Fig. 2. One can see that polarization values exceeding  $P \sim 0.5$  are reached already after 30 sec of pumping, and the ESR line corresponding to the  $b$ - $c$  transition is no longer detected in the noise after 20 min of pumping.

Due to the high  $Q$  of the FPR and the long spin-lattice relaxation time of the  $^{31}\text{P}$  electrons, the allowed  $b$ - $c$  transition is fully saturated in a fraction of a second. The DNP occurs due to the Overhauser effect, which transfers the population as  $b \rightarrow c \rightarrow a$ . It is clear that the DNP rate is limited by the much slower relaxation via the forbidden  $a$ - $c$  transition, characterized by a cross-relaxation time  $T_{ac}$ . Since the nuclear polarization can be negative (when  $n_a < n_b$ ), in order to check whether the DNP behaves exponentially, we plotted  $1 - P(t_p)$  in log units in Fig. 3. One can see that the polarization dynamics deviates strongly from an exponential at the beginning of the pumping. We verified that the ESR excitation power is strong enough to saturate the allowed transitions. Pumping dynamics

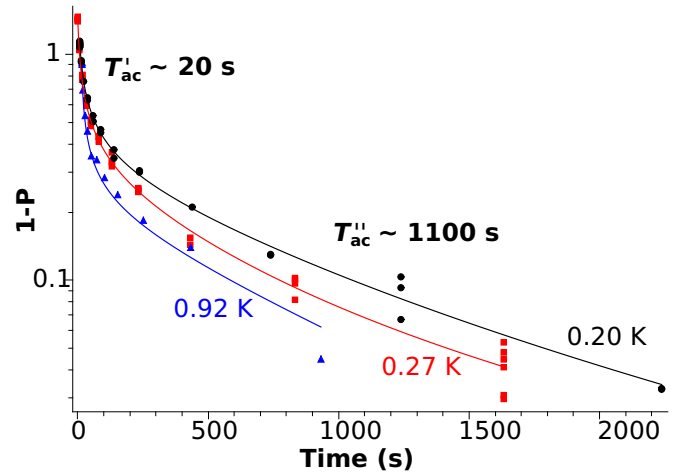


FIG. 3. (Color online) Dynamics of the DNP process via the Overhauser effect when pumping the  $b$ - $c$  transition.  $\log[1 - P(t)]$  is plotted as a function of pumping time  $t_p$  for 0.20 K, black dots; 0.27 K, red squares; and 0.92 K, blue triangles. The lines are guides for the eye.

did not depend on excitation power near its maximum value. We have not observed any reduction in the DNP efficiency after decreasing the power by 2–3 dB. Only attenuating it by more than 10 dB led to a decrease of the DNP. The characteristic time of the DNP buildup is  $T'_{ac} \approx 20$  s at the beginning and  $T''_{ac} \approx 1100$  s at the end, when the function is almost exponential. We estimate that the polarization  $P > 0.98$  was reached in this experiment, based on the signal-to-noise ratio of  $\approx 100$  since the  $b$ - $c$  ESR line vanishes in the noise after  $\approx 20$  min of pumping.

We repeated the  $b \rightarrow c$  pumping experiment at temperatures 0.2 K, 0.27 K, and 0.92 K and found for each case that the pumping dynamics follows a similar nonexponential dependence (Fig. 3). One can see that the DNP is built somewhat faster at higher temperatures. Above 1 K we could not reach very high DNP values even after pumping for very long time. This is explained by the enhanced nuclear relaxation at higher temperatures, as we shall consider below. Our results indicate that the temperature dependence of the flip-flop cross-relaxation rate is relatively weak. Pumping the  $b \rightarrow c$  transition one may think of another possible pathway for the DNP: via the nuclear relaxation between the upper hyperfine states:  $c \leftrightarrow d$ . In this case, the slowest process  $c$ - $d$  nuclear relaxation will mediate the DNP rate. However, as we shall see below, the nuclear relaxation rate is extremely slow below 1 K, in contradiction with our observations.

In the next experiment we pumped the  $a$ - $d$  transition with 32 MHz FM modulated excitation equivalent to a 11.4 G window in the ESR spectrum. In this case the Overhauser effect leads to the population transfer  $a \rightarrow d \rightarrow b$  which makes  $n_a < n_b$  and creates a negative DNP. A result of such experiment is shown in trace 4 of Fig. 2. The rate of the DNP process is substantially slower than in the previous experiment. The polarization was increased by a factor of 2 after about 10 h pumping. Since the DNP in this case is limited by the flip-flip relaxation, we estimate the corresponding relaxation time  $T_{bd} \approx 5 \times 10^4$  s,  $\gtrsim 50$  times larger than  $T'_{ac}$ .

One can also realize the solid effect (SE) DNP by pumping the forbidden  $a \rightarrow c$  or  $b \rightarrow d$  transitions. Displacements of

these transitions from the center of the ESR spectrum are given by the nuclear Zeeman energy and are  $\pm \approx 28.3$  G in the field of 4.6 T. This implies a well-resolved separation of 7.3 G from the center of  $^{31}\text{P}$  ESR lines, as shown in the lower trace of Fig. 2. These forbidden transitions are excited only by the parallel component of the RF field and their probabilities are reduced by  $\eta^2$  according to the first-order perturbation theory [6]. Since we do not have parallel component of the RF field in the TEM mode of the FPR, we expected that the SE cannot be realized in the present setup. However, we attempted such an experiment. We stopped magnetic field at the position of the  $a \rightarrow c$  transition (marked by the dashed line in Fig. 2) and applied maximum RF power for 1.5 hours. We used a smaller FM modulation of 1 MHz (0.36 G) to increase the excitation rate. We have not observed changes in the  $^{31}\text{P}$  ESR spectrum after such pumping. After further decrease of the FM to 100 kHz, some small hole in the  $a$  line and a corresponding peak, barely visible within the noise, appeared at the position of the  $b$  line. This implies that the forbidden transition probabilities are nonzero, and the first-order perturbation theory is not sufficient to evaluate them. The SE could be realized using the transversal RF field, if higher ESR powers would be available. Note that the experiment on negative DNP by pumping the  $a-d$  transition mentioned above cannot be influenced by the SE effect. Using 32 MHz modulation, only a small part of the wing of the forbidden line falls into the edge of the pumping window (see Fig. 2). This confirms that the DNP effect observed after pumping the  $a$  line is solely due to the OE.

### B. Nuclear relaxation of $^{31}\text{P}$

Monitoring the nuclear polarization after the DNP experiments described in the previous section, we have not observed any changes of  $P$  within several days of observations if the sample temperature was kept below 0.5 K. However, at temperatures above 1 K, weak signals from the  $b-c$  line were observed even after pumping it for a very long time  $t_p \gg T_{ac}''$ . Since the nuclear  $a-b$  relaxation is a mechanism competing with DNP, this process can be responsible for the decrease of the maximum DNP value observed at higher temperatures. To verify this, the nuclear  $a-b$  relaxation was studied as a function of temperature. We transferred all or a part of the  $b$ -state population into  $a$  state by pumping the  $b-c$  ESR line as described above. This determined the starting value of polarization  $P_0$  for relaxation measurements. At this stage the temperature was kept at the lowest value of 0.2 K, so that nuclear relaxation was negligible. Then, the sample cell was rapidly warmed up and the temperature was stabilized to a desired value between 0.75 and 2.2 K. The evolution of the spin states towards the thermal equilibrium was monitored by measuring repeatedly the ESR spectrum with the low detection power. Results of nuclear relaxation measurements are demonstrated in Fig. 4 for  $T = 1.37$  K and different values of  $P_0$ .

First we measured relaxation starting from the maximum polarization  $P \approx 1$ , and followed its evolution for long enough time until it approached its value at thermal equilibrium  $\approx 0$ . One can see (upper curve in Fig. 4 and the insert) that the relaxation does not decrease exponentially. Similarly to the DNP evolution reported in the previous section, the process

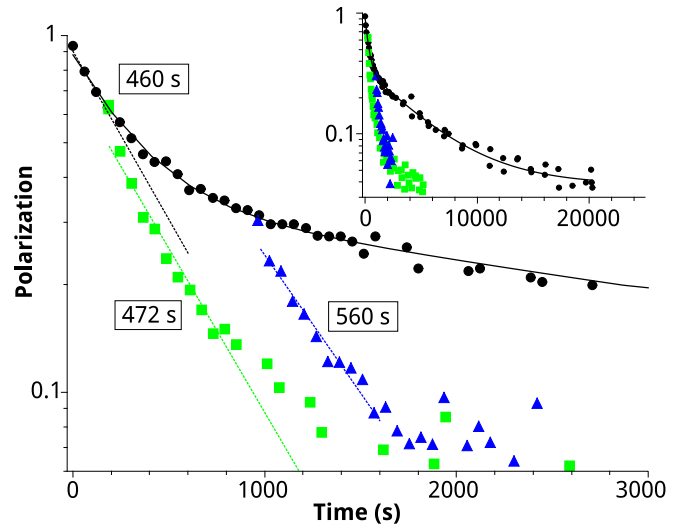


FIG. 4. (Color online) Nuclear relaxation measured with different starting polarization values at 1.37 K. Black dots, relaxation curve after starting with  $P_0 \approx 1$ ; green squares and blue triangles, relaxation curves with lower starting values of  $P_0 \approx 0.6$  and  $P_0 \approx 0.3$ . The solid line is a biexponential fit to the data. The dashed lines are exponential fits to the initial parts of the data. The data for  $P_0 \approx 0.6$  and  $P_0 \approx 0.3$  are shifted in time to match the starting points with the  $P_0 \approx 1$  curve. The inset shows full time range of the relaxations.

is substantially faster in the beginning. A biexponential fit to the data gives a better result, and provides two time constants: short  $T_{ab}'$  and long  $T_{ab}''$ .

In a further study of the biexponential relaxation, we made measurements in which we studied how the relaxation rate depends on the polarization history, or on the starting polarization. In the end of the previous measurement, when the low value  $P \approx 0.03$  was reached, we pumped the  $b-c$  transition for a short time (30–50 s). As a result, the nuclear polarization was enhanced to medium value  $P_0 \approx 0.6$ . The subsequent nuclear relaxation measurement revealed that the relaxation rate is much larger than it was at the same  $P$  value in the previous measurement, starting with  $P_0 \approx 1$ . A similar result was found after repeating this measurement for an even smaller starting polarization ( $P_0 \approx 0.3$ ). The slopes of the relaxation curves were quite the same in the beginning, meaning that the  $T_{ab}'$  does not depend on the starting value of the nuclear polarization.

The relaxation rates  $1/T_{ab}'$  and  $1/T_{ab}''$  as functions of the inverse temperature are presented in Fig. 5. Both relaxation rates follow an exponential dependence on  $\Delta/k_B T$ . A fit to the data gives  $\Delta/k_B = 5.9(7)$  K. For comparison we also included in Fig. 5 results of Ref. [9] obtained in strong (8.6 T) magnetic field. The results presented in this work reveal a single exponential behavior of relaxation, which is not surprising since at temperatures above 3.5 K used in their work, the short relaxation time  $T'$  is too short to be measured. However, the data of Ref. [9] confirm qualitatively the same mechanism of nuclear relaxation.

### C. DNP of $^{29}\text{Si}$

The ESR technique allows easy measurement of the phosphorus hyperfine state populations, which are

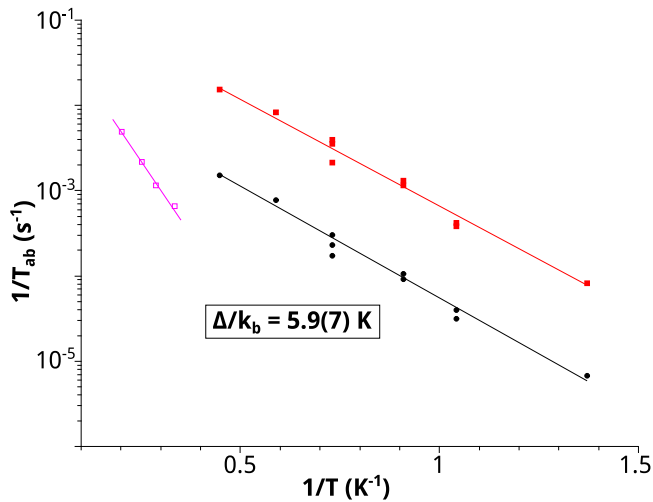


FIG. 5. (Color online) Nuclear relaxation rates  $1/T'_{ab}$  (filled squares) and  $1/T''_{ab}$  (black dots) as a function of inverse temperature and exponential fits to the data. Data of van Tol *et al.* [9] are given as open squares for comparison.

proportional to the integrals of the absorption signal. Unfortunately, the  $^{29}\text{Si}$  polarization cannot be measured with the same method. Some information, however, can be extracted from the ESR spectra. If all the  $^{29}\text{Si}$  nuclei are polarized, the superhyperfine interaction shifts the ESR lines in respect to the lines with unpolarized spin states. The sign of the shift depends on the polarization direction of  $^{29}\text{Si}$ . As an example, we consider a splitting of the donor electron spin levels by superhyperfine interaction with one  $^{29}\text{Si}$  nucleus, shown in Fig. 6. The spin orientations of the  $^{29}\text{Si}$  level scheme are opposite to the  $^{31}\text{P}$  levels due to the negative gyromagnetic ratio of  $^{29}\text{Si}$  and the splitting of the levels are smaller because of the weak superhyperfine interaction ( $\lesssim 3$  MHz [1]). Saturating the whole ESR line of  $^{31}\text{P}$ ,  $b$ - $c$  for example, induces simultaneously transitions  $b_+$ - $c_+$  and  $b_-$ - $c_-$ , with opposite

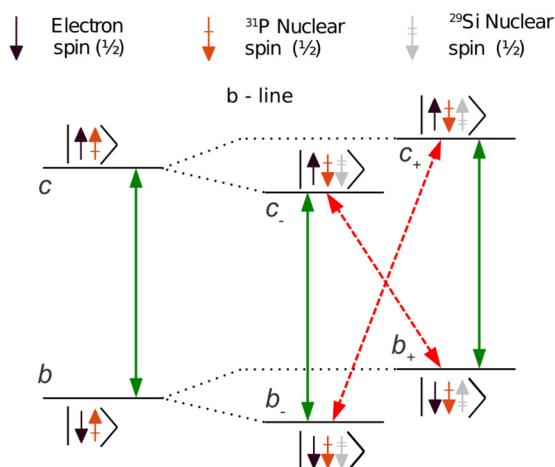


FIG. 6. (Color online) Hyperfine levels of P donor split by superhyperfine interaction with one  $^{29}\text{Si}$  nucleus. The solid arrows indicate the allowed transitions and dashed arrows indicate the forbidden transitions.

directions of the  $^{29}\text{Si}$  spins involved (denoted with + or - subscripts in Fig. 6). The states  $b_+$  and  $c_-$  are mixed and they have opposite directions of the electron and  $^{29}\text{Si}$  nuclear spins. Saturating the ESR line creates OE DNP of the  $^{29}\text{Si}$  in a similar way to that in the original Overhauser experiment for nuclei in metals. During the pumping the populations are transferred in both ways:  $b_- \rightarrow c_- \rightarrow b_+$  and  $b_+ \rightarrow c_+ \rightarrow b_-$ . As a result the  $^{29}\text{Si}$  spin populations are redistributed between  $b_+$  and  $b_-$  states. Due to the higher rate of the flip-flop transition most of the  $^{29}\text{Si}$  spins end up in the  $b_+$  state. Since the resonant field for the  $b_+$ - $c_+$  transition is larger, the ESR line will acquire shift to the right. The magnitude of the shift can be estimated numerically by arranging the 4.7% of  $^{29}\text{Si}$  nuclei randomly into the lattice sites and taking into account known values of hyperfine interactions for each site [12–14]. We performed such evaluation and for fully polarized sample obtained a predicted shift of  $\approx 2.8$  G.

In the DNP experiments described in Sec. III the  $^{31}\text{P}$  allowed transitions were pumped for long times, leading to the population transfer from  $a$  to  $b$  state and vice versa. The relaxation time of the  $^{29}\text{Si}$  nuclear spins is expected to be very long at temperatures of  $\sim 1$  K. Therefore, it was difficult to trace the possible shift of the spectrum due to the  $^{29}\text{Si}$  polarization. Therefore, we tried to depolarize the sample by applying RF excitation at 38.9 MHz, resonant with the NMR transition of  $^{29}\text{Si}$ , and driving its polarization back to zero. The change in the spectra resulting from the depolarization is presented in Fig. 7. The upper trace, recorded for the sample with maximum polarization, is shifted to the right from the unpolarized (lower) trace by  $\approx 2.6$  G. This is very close to the maximum predicted shift of 2.8 G, and we evaluate that polarization of  $^{29}\text{Si}$  exceeding 60% was reached in this work. To our knowledge this is the highest polarization reached in this system.

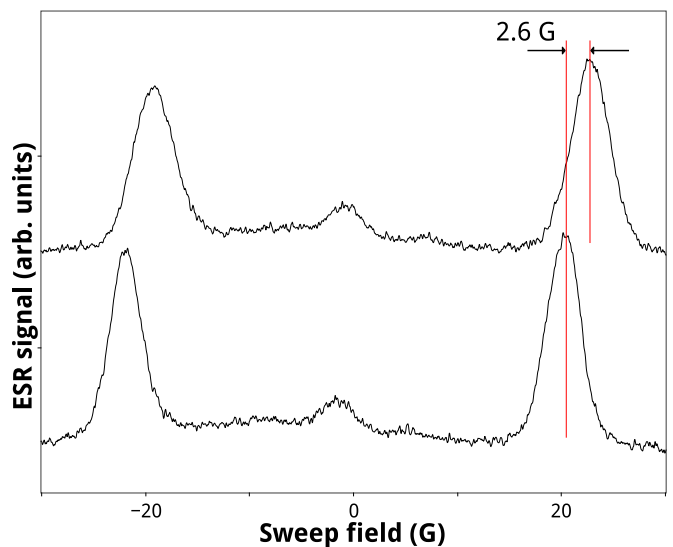


FIG. 7. (Color online) Shift of the P ESR lines due to polarization of  $^{29}\text{Si}$ . Upper trace: The sample with maximum polarization. Lower trace: After depolarization by applying frequency-modulated RF excitation at the frequency of  $38.9 \pm 3$  MHz, corresponding to the NMR transitions of  $^{29}\text{Si}$  in 4.6 T field.

## IV. DISCUSSION

### A. Relaxation rates

The rate of DNP via the Overhauser effect is defined by the probabilities of the flip-flop and flip-flip transitions  $1/T_{ac}$  and  $1/T_{bd}$ . There are two main relaxation mechanisms relevant to our conditions: relaxation due to the oscillating internal magnetic fields caused the agitation of the lattice (dipolar relaxation), and the thermal modulation of the magnetic hyperfine interaction (hyperfine relaxation) [6,15]. In strong magnetic fields the rate of dipolar relaxation is reduced by the hyperfine mixing factor squared  $\eta^2$ , making this channel negligible. Then, the hyperfine relaxation dominates, and the order of magnitude evaluation of the relaxation time constant can be done using the equation [15]

$$T_x \equiv T_{ac} = \frac{4\pi \hbar^2 \rho}{\gamma_e^2 B_0^2 k T \gamma^2 A}, \quad (1)$$

where  $\gamma$  is a numerical factor between 10 and 100, and  $\rho$  is the density of silicon. Note that the relaxation rate due to this mechanism increases as  $B_0^2$  as a function of magnetic field in contrast to the dipolar relaxation. Relaxation rates were found to be independent of the donor concentration [10] up to  $3 \times 10^{16} \text{ cm}^{-3}$ , which is only a factor of 2 lower than used in this work.

For Si:P in 0.3 T (0.8 T) field and temperature of 1.2 K Eq. (1) gives  $T_x = 3.4 \times 10^4 \text{ s}$  ( $0.5 \times 10^4 \text{ s}$ ), which agrees within an order of magnitude with the experimental results of Feher and Gere [12]  $T_x \approx 10^5 \text{ s}$  in 0.32 T field and  $T_x \approx 1.8 \times 10^4 \text{ s}$  in 0.8 T field and temperature of 1.25 K. We would like to note also that these two values confirm the  $1/B_0^2$  dependence of the relaxation time. If we now extrapolate the data of Ref. [12] to our field of 4.6 T and temperature of 0.75 K, we get  $T_x \approx 10^3 \text{ s}$  which is in good agreement with our experimental data for  $T_{ac}'' \approx 1100 \text{ s}$ . So, the phonon-induced modulation of the hyperfine interaction [15] can explain the values of the long cross-relaxation time  $T_{ac}''$  observed in this work. However, the fast cross relaxation with  $T_{ac}' \approx 20 \text{ s}$  in the beginning of the DNP cannot be explained by the theory involved so far.

The observed biexponential behavior can be explained if we consider the effect of the neighboring  $^{29}\text{Si}$  on the P cross relaxation. The 4.7% randomly distributed magnetic nuclei of  $^{29}\text{Si}$  create anisotropy in the hyperfine interaction of P with its own nucleus. This leads to a strong enhancement of the forbidden relaxation rates, especially for the donors which have one or more  $^{29}\text{Si}$  in the closest lattice shells. For these  $^{29}\text{Si}$  nuclei the anisotropic dipole-dipole interaction with donor electron leads to a fast nuclear relaxation, which scales as  $1/r^6$  with the distance between the donor and the  $^{29}\text{Si}$  nucleus [16,17]. In a similar fashion the proximity of  $^{29}\text{Si}$  may lead to enhancement of the  $^{31}\text{P}$  cross relaxation. We can distinguish two groups of donors: group I, having one or several  $^{29}\text{Si}$  in the nearest lattice sites with strong hyperfine interactions, and group II, not having  $^{29}\text{Si}$  nuclei nearby. The neighbors with strongest hyperfine interactions are in the [400] (6 nuclei) and [440] (12 nuclei) lattice sites [13]. For all other neighbors the interactions are substantially weaker. One may evaluate the probability of not having a single  $^{29}\text{Si}$  in either of [400] sites

as  $P_{II} = (1 - 0.047)^6 \approx 0.75$ , or  $P_{II} \approx 0.42$  for not having it in either of 18 above mentioned sites. This means that the number of  $^{31}\text{P}$  in the group I can be of the same order as in the group II. The group I donors have an enhanced cross relaxation and faster DNP rate, which is seen in the first part of the polarization dynamics of Fig. 3. Once these nuclei get fully polarized, the DNP proceeds more slowly with the donors in the group II, and in this case the observed characteristic time  $T_{ac}''$  should be about the same as for the P in isotopically purified  $^{28}\text{Si}$ .

One of the nuclear relaxation mechanisms in insulating solids, the nuclear Orbach process [7], proceed via the upper hyperfine states and the flip-flop and flip-flip cross relaxation transitions. The temperature dependence of the nuclear relaxation rate in this case is given by the Boltzmann factor:

$$\frac{1}{T_{ab}} = e^{-\hbar\gamma_e B/k_B T} \left( \frac{1}{T_{ac}} + \frac{1}{T_{bd}} \right). \quad (2)$$

This means that the nuclear relaxation of the  $^{31}\text{P}$  atoms of the group I donors should be also faster and could explain our observation of the two time scales in the nuclear relaxation measurements (Figs. 4 and 5).

### B. Polarization of $^{29}\text{Si}$

In the silicon of normal isotope composition, the  $^{29}\text{Si}$  nuclear spins play an important role in the spin dynamics of shallow donors [18–20]. The polarization transfer between different nuclei is a well-known effect [21]. The  $^{29}\text{Si}$  nuclear spins are also getting polarized during the DNP experiments with  $^{31}\text{P}$ . The polarization of the  $^{29}\text{Si}$  nuclei in the neighboring lattice sites around the donors may lead to the enhancement of the cross relaxation of  $^{31}\text{P}$  in the initial part of the DNP curve (Fig. 3), and also accelerate nuclear relaxation just after pumping. In other words, the forbidden relaxation time  $T_{ac}'$  may depend on the polarization of  $^{29}\text{Si}$ , which is created simultaneously with the OE DNP of phosphorus. This influences the fast-relaxing group I donors, and should not affect  $T_{ac}''$  and  $T_{gb}''$ .

The rate of  $^{29}\text{Si}$  DNP is highest for the nuclei closest to the donors. However, due to fast spin diffusion the polarization rapidly propagates into the bulk of the sample [16]. The rate of the spin diffusion is substantially slower inside the so-called spin diffusion barrier [16,20] which is about 10 nm around P donors in our case, and is comparable to the  $\approx 25 \text{ nm}$  mean distance between the donors. After switching off the pumping, the nearest  $^{29}\text{Si}$  will get depolarized by the donors. The polarization outside the diffusion barrier may decay only because of the nuclear relaxation, which is very slow for remote, noninteracting  $^{29}\text{Si}$ . Therefore, the  $^{29}\text{Si}$  nuclear polarization may be rather inhomogeneous during the relaxation measurements. However, since the diffusion barrier is effectively removed during pumping, when the electron spins are depolarized, we expect that the high bulk polarization of  $^{29}\text{Si}$  has been obtained immediately after the pumping.

### C. Efficiency of DNP

It is well known from the theory of the Overhauser effect [22], that in the high-temperature limit ( $g_e\mu_B B \ll k_B T$ ) the DNP enhancement over the thermal polarization is given by the ratio of the electron and nuclear gyromagnetic ratios  $\gamma_e/\gamma_N$ , which is  $\approx 1600$  for  $^{31}\text{P}$ . However, the polarization enhancement is not a good merit of the DNP efficiency in high fields and low temperatures, when the polarization approaches very close to 1. We think that it is better to consider the ratio of the hyperfine populations  $n_a/n_b$  for evaluation of the DNP efficiency, which we will use below.

In the general case the equations for hyperfine state populations due to OE can be found in the textbooks [7]. Here we present the results in the case of long nuclear relaxation time  $T_{ab} \gg T_{ac}$  and low temperatures  $\hbar\gamma_e B \gg k_B T$ , which can be obtained from the following simple considerations.

A microwave excitation saturating fully the electronic  $b$ - $c$  transition for a long enough ( $t_p \gg T_{ac}$ ) time will establish thermal equilibrium between  $a$  and  $c$  states and therefore  $n_b = n_c \approx n_a \exp(-\hbar\gamma_e B/k_B T)$ . After switching off the pumping, all the atoms in the  $c$  state will quickly relax to the  $b$  state, and we get the relation

$$\left(\frac{n_a}{n_b}\right)_{\text{DNP}} = \frac{n_a}{2n_c} = \frac{1}{2} e^{\frac{g_e\mu_B B}{k_B T}}. \quad (3)$$

At 4.6 T and 0.2 K this gives a theoretical limit of the Overhauser DNP:  $n_a/n_b \approx 10^{13}$ .

So far we have neglected the nuclear relaxation, which will transfer atoms back from the  $a$  to  $b$  state reducing the nuclear polarization. If the DNP rate is balanced by the nuclear relaxation and  $n_a \gg n_b$ , then in a steady state

$$\frac{dn_a}{dt} = \frac{n_c}{T_{ac}} - \frac{n_a}{T_{ab}} = 0, \quad (4)$$

which gives the maximum value for the nuclear populations limited by the  $a$ - $b$  nuclear relaxation,

$$\left(\frac{n_a}{n_b}\right)_{\text{max}} = \frac{n_a}{2n_c} = \frac{T_{ab}}{2T_{ac}}. \quad (5)$$

The temperature dependence of our data for the short and long relaxation times (Fig. 5) can be well fitted by the exponential dependence of Eq. (2), with the exponent  $\Delta/k_B = 5.9(7)$  K being close to  $\hbar\gamma_e B/k_B \approx 6.2$  K. In the temperature range of this work the forbidden relaxation time has very weak temperature dependence, which can be neglected. Therefore from Eqs. (5) and (2) it follows that the maximum polarization, limited by the nuclear relaxation, has the same temperature dependence as that for the theoretical limit of Overhauser DNP [Eq. (3)]. Taking the pre-exponent of  $T_{ab}''$  from the fit to our data, we found that the effect of the nuclear relaxation is to reduce maximum polarization by two orders of magnitude from the theoretical limit of the Overhauser DNP [Eq. (3)]. At  $T = 0.2$  K we evaluate from Eq. (5) that an extremely pure spin system with  $n_a/n_b \approx 5 \times 10^{11}$  can be created after sufficiently long pumping. Reaching very high values of the DNP then actually becomes only a matter of time at these conditions. Pumping for a couple of hours ( $t_p \sim 7T_{ac}''$ ) will increase  $n_a/n_b$  by three orders of magnitude. The DNP can be done with very low values of the pumping power, enough to fully saturate the allowed ESR transitions, which is less than  $1 \mu\text{W}$  in our case.

In summary, from the evolution of the spin polarization during the DNP and the nuclear relaxation measurements, we conclude that the polarization of neighboring  $^{29}\text{Si}$  spins has an important role in the dynamics of the  $^{31}\text{P}$  nuclear spins. Pumping the allowed ESR transition leads to the effective DNP of both nuclear ensembles. The populations of the phosphorus hyperfine states were measured directly by ESR. Record high polarization values were reached after pumping with small excitation power and for relatively short times. We believe that the possibility of creating ultrapure ensembles of nuclear spin states demonstrated in this work may find useful applications, e.g., in the field of quantum computing.

### ACKNOWLEDGMENTS

We would like to thank K. Itoh, K. Kono, D. Konstantinov, S. Lyon, and A. Tyryshkin for useful discussions. We acknowledge funding from the Wihuri Foundation and the Academy of Finland Grants No. 260531 and No. 268745. S. S. thanks UTUGS for support.

- 
- [1] G. Feher and E. A. Gere, *Phys. Rev.* **103**, 501 (1956).
  - [2] B. E. Kane, *Nature (London)* **393**, 133 (1998).
  - [3] T. Maly, T. Debelouchina, V. S. Bajaj, Kan-Nian Hu, Chan-Gyu Joo, M. L. Mak-Jurkauskas, J. R. Sirigiri, P. C. A. van der Wel, J. Herzfeld, R. J. Temkin, and R. G. Griffin, *J. Chem. Phys.* **128**, 052211 (2008).
  - [4] V. A. Atsarkin, *J. Phys.: Conf. Ser.* **324**, 012003 (2011).
  - [5] A. Abragam, *Phys. Rev.* **98**, 1729 (1955).
  - [6] C. D. Jeffries, *Phys. Rev.* **117**, 1056 (1960).
  - [7] A. Abragam and M. Goldman, *Nuclear Magnetism: Order and Disorder* (Clarendon Press, Oxford, 1982), Chap. 6.
  - [8] D. G. Crabb and W. Meyer, *Annu. Rev. Nucl. Part. Sci.* **47**, 67 (1997).
  - [9] J. van Tol, G. W. Morley, S. Takahashi, D. R. McCamey, C. Boehme, and M. E. Zvanut, *Appl. Magn. Reson.* **36**, 259 (2009).
  - [10] A. Honig and E. Stupp, *Phys. Rev.* **117**, 69 (1960).
  - [11] S. Vasiliev, J. Järvinen, E. Tjukanoff, A. Kharitonov, and S. Jaakkola, *Rev. Sci. Instrum.* **75**, 94 (2004).
  - [12] G. Feher and E. A. Gere, *Phys. Rev.* **114**, 1245 (1959).
  - [13] E. Hale and R. Miehler, *Phys. Rev.* **184**, 739 (1969).
  - [14] J. L. Ivey and R. L. Miehler, *Phys. Rev. B* **11**, 849 (1975).

- [15] D. Pines, J. Bardeen, and C. Slichter, *Phys. Rev.* **106**, 489 (1957).
- [16] N. Bloembergen, E. M. Purcell, and R. V. Pound, *Phys. Rev.* **73**, 679 (1948).
- [17] W. E. Blumberg, *Phys. Rev.* **119**, 79 (1960).
- [18] H. Hayashi, T. Itahashi, K. Itoh, L. Vlasenko, and M. Vlasenko, *Phys. Rev. B* **80**, 045201 (2009).
- [19] A. E. Dementyev, D. G. Cory, and C. Ramanathan, *Phys. Rev. Lett.* **100**, 127601 (2008).
- [20] C. Ramanathan, *Appl. Magn. Reson.* **34**, 409 (2008).
- [21] I. Solomon, *Phys. Rev.* **99**, 559 (1955).
- [22] C. Slichter, *Principles of Magnetic Resonance* (Springer-Verlag, 1990), 3rd ed., pp. 254-257.